The 2009 IEEE/RSJ International Conference on
Intelligent Robots and Systems
October 11-15, 2009 St. Louis, USA

Three-Layer Control for Active Wrists in Robotized Laparoscopic Surgery

E. Bauzano, V.F. Muñoz, I. Garcia-Morales, and B. Estebanez

Abstract— **This paper is focused on the motion control problem for a laparoscopic surgery robot assistant with an actuated wrist. These assistants may apply non-desired efforts to the patient abdomen. Therefore, this article proposes a control methodology based on three feedback levels, which have been defined as layers. These layers control different aspects of the endoscope movement. A low level assures the dynamic of the robot assistant is performed accordingly. The mid level emulates a passive wrist behavior to avoid any efforts over the abdomen. An external high level deals with the global movement planning. This architecture also makes easier to analyze the stability of the whole system. Finally, a real in-vitro experiment has been implemented with an industrial robot in order to contrast the validity of this article procedure.**

I. Introduction

MINIMALLY invasive surgery is based on making little incisions in the skin, in order to access the abdominal cavity with special long instruments. In this kind of procedures, an assistant is needed to manage the laparoscopic camera, which shows the abdominal cavity to the surgeon through a screen. This technique aims to reduce the size of the incisions in order to lessen patients' recovery time and limit any post-operative complication [1]. However, the disadvantage of this kind of surgery lies in the form of new limitations for the surgeon: movement restrictions, loss of touch and 3D perception, and hand-eye coordination problems. In this way, freedom can be improved by surgeon assistance in the form of new procedures based on robotic engineering.

One of the challenges arisen by the use of these technologies consists of replacing the surgeon assistant used in laparoscopic surgery procedures for moving the camera. The assistant task is to focus the camera on the area of interest for the main surgeon. Due to the assistant's steady hand, the endoscope may come into contact with a tissue, fail to center the area required by the surgeon or transmit unstable pictures to the monitor. The solution for these related problems is to design a robotic assistant for laparoscopic surgery.

A robotic assistant must locate the endoscope inside the abdominal cavity, so it points at the desired internal anatomical structure. This concept is known as *laparoscopic navigation*.

The endoscope point of insertion I_0 (fulcrum point) has a reference system attached (see Fig. 1), whose axes match with the robot axes base reference frame. The first one is used in order to specify the camera relative location through spherical coordinates α (*orientation angle*), β (*altitude angle*) and ρ (*external distance*, or distance from the wrist to the fulcrum point) [2]-[3]. Thus, the endoscope movements are described in terms of spherical coordinates.

A robotic assistant must be equipped with a wrist able to develop the spherical movements described above. In this way, possible solutions for this purpose are *passive* or *active wrists*. The first one consists of a mechanism with no actuated joints [4]-[6], so that it guarantees no efforts are applied to the abdominal wall. However, the endoscope location precision decreases with any uncertainty concerning the fulcrum knowledge.

The accuracy of the endoscope location can be improved by means of an active wrist, since it avoids the backlash between the endoscope and the trocar. However, this kind of structure can exert undesired forces to the abdominal wall. In this way, some works like Da Vinci [7] or AESOP [8], solve this problem by using a wrist with a remote rotation centre configuration [9]-[10], or with spherical arc wrists [11]. However, this kind of mechanic structures presents some drawbacks: they require special instruments for their implementation, a previous calibration procedure, and they are implemented via voluminous mechanisms.

Because of these limitations, this paper has been focused on direct actuated wrists [12]. Section II introduces the problem of laparoscopic navigation for direct actuated wrists, as well as the proposed motion control architecture. Section III is devoted to design an appropriate control

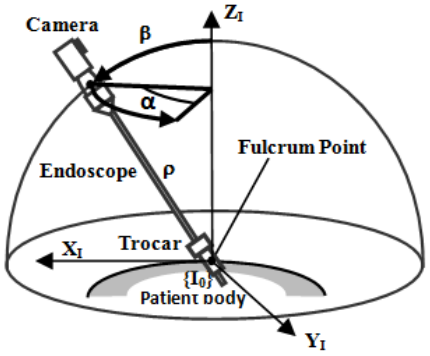

Fig. 1. Navigation of the laparoscopic camera on spherical coordinates.

Manuscript received March 1, 2009. This work was supported in part by the Spanish National projects DPI2007-62257 and the Regional one P07-TEP-02897.

V. F. Muñoz is with the System Engineering and Automation Department, University of Malaga, Spain (corresponding author to provide phone: +34 952 13 25 40; fax: +34 952 13 14 13; e-mail: vfmm@uma.es).

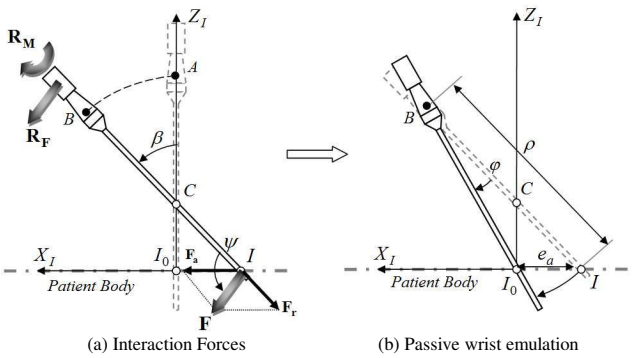

(a) Interaction Forces (b) Passive wrist emulation

Fig. 2. Endoscope-Abdomen interaction efforts (a) and passive wrist emulation control strategy (b).

strategy to solve the motion control problem, by means of passive wrist emulation. Section IV details the stability of the control system. Section V shows an *in-vitro* experiment with the proposed control strategy. Finally, section VI concludes the advantages of using direct actuated wrists, as well as possible future applications related to minimally invasive surgery.

II. Fundamentals on Laparoscopic Navigation

This section describes the navigation problem of the endoscope. Direct actuated wrists avoid the backlash introduced by the trocar-endoscope interaction which appears on passive wrists solutions. Thus, the endoscope always reaches the desired spherical position in spite of inaccurate estimation of the fulcrum. However, this uncertainty will eventually force the abdominal wall and could damage the patient.

Firstly, an analysis of the endoscope interaction with the abdominal wall during the navigation is presented. Then, this section will propose a control strategy whose goal is to decrease the efforts applied to the abdomen. With this information, a global control architecture scheme will be introduced to explain the problem of laparoscopic navigation and the solution proposed in this paper.

A. Actuated wrists navigation problem

Fig. 2 (a) illustrates an endoscope movement where the altitude angle β changes from a starting null position A to a final position B. The robot movement planner uses an initial estimation of the fulcrum position C for computing the arc shape trajectory, instead of the unknown real one I_0. This situation involves that the endoscope exerts an undesired force to the abdominal wall, $\mathbf{F_a}$, in such a way that the fulcrum point is moved from I_0 to a new position I. On the other hand, the endoscope slides through the trocar, producing a friction force $\mathbf{F_r}$. In the figure, $\mathbf{F}$ represents the nominal force applied to the abdominal wall, defined as the composition of $\mathbf{F_a}$ and $\mathbf{F_r}$. Finally, let be $\mathbf{R_F}$ and $\mathbf{R_M}$ the force and torque measured at the camera reference frame.

The abdominal force $\mathbf{F_a}$ gives information about the direction where the fulcrum point I is displaced. Therefore, this force is used for two purposes: i) if navigation is being performed in an accurate way, and ii) any unexpected change implies a fulcrum location variation (i.e. respiratory motion or abdominal cavity air pressure variation).

A null fulcrum point estimation error (i.e. $\|I_0, C\|=0$) implies that no efforts are applied to the abdominal wall, and therefore the fulcrum point keeps its initial position (i.e. $I_0=I$). A similar analysis can be deduced from an orientation angle α.

B. Control Strategy

The proposed approach to reduce the efforts applied to the abdominal wall is based on emulating the passive wrist behaviour. This way, on the situation shown in Fig. 2 (a), a non-actuated wrist would keep its orientation according to the initial position at the fulcrum point I_0. Fig. 2 (b) shows this passive compliance by means of the angle φ. Thus, the motion controller of the direct actuated wrist must compute this compensation angle φ to get the desired behavior.

As described above, the angle φ is required in order to orientate the endoscope accordingly to the initial fulcrum point I_0. Let be e_a the distance between I and I_0, as a consequence of the altitude movement β shown in Fig. 2 (a). The compensation angle φ is related to e_a, from a geometrical point of view, by means of the expression (1).

$$e_a = \frac{\rho \tan\varphi}{\cos\beta\left(1+\tan\beta\tan\varphi\right)} \tag{1}$$

Expression (1) can be simplified when values of φ are considered closed to zero, as shown in the relationship (2).

$$e'_a = \frac{\rho}{\cos\beta}\varphi \tag{2}$$

Fig. 3 shows the e_a computation error due to the use of the simplified expression (2). This figure presents a set of curves corresponding to different values of the altitude angle β, when the external distance ρ value is the maximum possible (ρ=230mm). Each single curve details the evolution of the mentioned error ($e_a - e'_a$) when the compensation angle φ increases. The passive wrist emulation (from now, PWE)

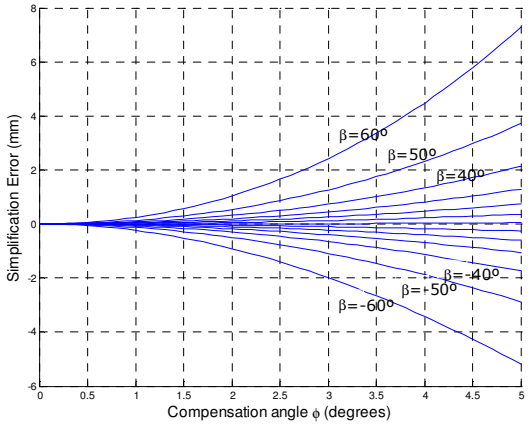

Fig. 3. Approximation error between e_a and e'_a.

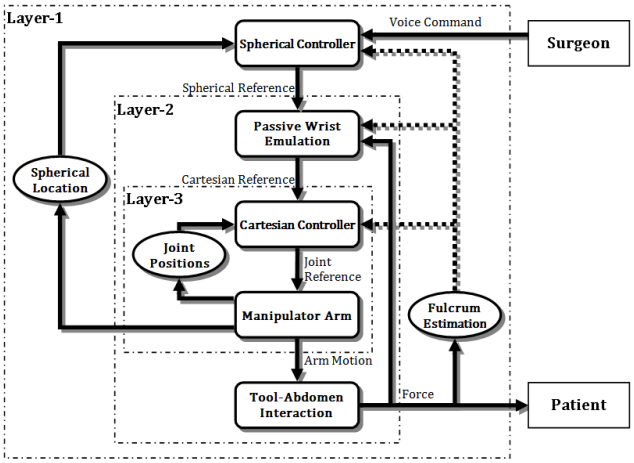

Fig. 4. Architecture scheme for the laparoscopic navigation problem with actuated wrists.

algorithm uses an empirical threshold for φ equal to 2 degrees in order to bound the computation error of e_a below 1 millimeter.

As it can be noticed from Fig. 2 (b), the PWE control action, by means of φ, changes the altitude angle of the endoscope. In this way, an external spherical control loop is needed in order to recover the desired goal altitude β. Moreover, the dynamic behaviour of the PWE must be fast enough in order to reach the compensation angle φ before the spherical control loop commands the next altitude goal.

C. Architecture Scheme

This subsection presents the three layers architecture scheme proposed in order to control the movements of a direct actuated wrist robotic assistant (see Fig. 4). The proposed methodology divides the laparoscopic navigation problem into three less complex actions, in such a way that simplifies the stability analysis of the overall system.

The scheme includes the external spherical control loop, marked as Layer-1, and the passive wrist emulation control strategy (Layer-2) described at subsection II.B. Moreover, an inner Cartesian control layer (Layer-3) is added in order to assure the Cartesian trajectory tracking.

This cascade control scheme makes easier the stability study of the overall system, since it is possible to prove the stability of each layer in an isolate mode. This question will be detailed in section IV.

In this way, the surgeon sends the endoscope spherical goal coordinate to the spherical controller. This control loop feeds back both the current endoscope spherical location and the force and torque readings provided by a force sensor attached to the robot wrist. The goal spherical coordinate is reached by means of this layer in spite of the orientation or altitude changes introduced by the passive wrist emulation. This emulation was described in Fig. 2 (b) and it uses the force sensor feedback in order to carry out its action. Finally, the Cartesian controller tracks the desired spherical trajectory.

Moreover, this cascade architecture is designed in such a way that the inner control loop is in steady state when the outer one sends the next reference to it. Consequently, the control period of each Layer must be at least five times greater than the time constant of its inner layer.

III. Control Layers

This chapter studies the control law of each layer explained in section II.C. The explanation will use the altitude angle β, however similar conclusions can be deduced for the orientation angle α.

A. Internal Layer: Cartesian Controller

The influence of this Layer is essential in order to reduce the robot dynamic to a first order behaviour. Both, a trajectory Cartesian planner and a control scheme based on the inverse Jacobian matrix, are used to guarantee such dynamic on the robot movements (see Fig. 5).

The Cartesian planner computes a smooth trajectory by using an endoscope spherical reference, defined by an arc length L_r and a wrist orientation γ_r, for making the conversion of this spherical reference into a Cartesian one.

On the other hand, the Cartesian loop implements a control law based on the inverse of the Jacobian shown in the expression (3).

$$\dot{\theta}_r = J^{-1}(\theta)(K_X \overline{X} + \dot{X}_r) \tag{3}$$

In this expression, $\dot{X}_r$ is the desired velocity, $\overline{X}$ is the difference between the desired and actual location given by the function $F(\theta)$ after feeding back the joints vector θ, K_X a constant which defines the Cartesian trajectory tracking dynamic, $J^{-1}(\theta)$ the inverse of the Jacobian matrix, and $\dot{\theta}_r$ the joints references.

The low-level joints control consists of velocity PID controllers, adjusted to give a first order output with a unitary gain and a constant time as low as possible. Also, the control period T_3 of this Cartesian controller must be lower than external layers, in order to read the robot joints when they are already stable. Under these circumstances, the Cartesian control loop obeys the expression (4).

$$\dot{\theta}(kT_3 + T_3) = \dot{\theta}_r(kT_3) \tag{4}$$

This situation establishes that the dynamic error (3) on the followed trajectory is zero (5).

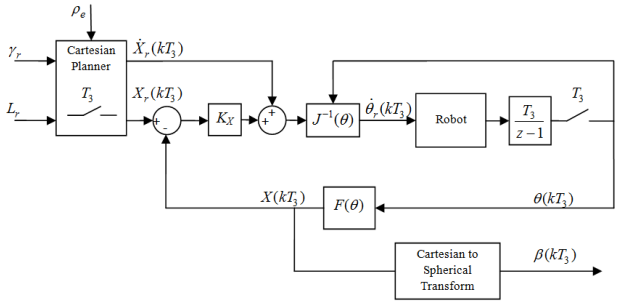

Fig. 5. Cartesian controller.

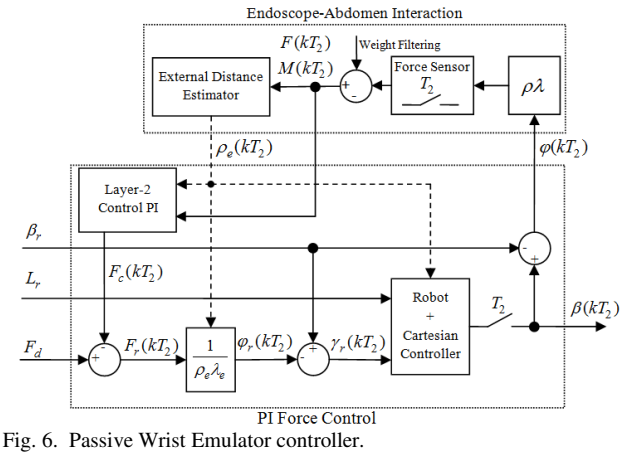

Fig. 6. Passive Wrist Emulator controller.

$$K_x\overline{X} + \dot{\overline{X}} = 0 \tag{5}$$

This expression defines the dynamic error when it tends asymptotically to zero with the K_X parameter, where $\dot{\overline{X}}$ is the difference between the desired and actual Cartesian velocity.

As a conclusion, a reduced control period assures that position and velocity references are followed. On the other hand, from a continuous system point of view, the followed error will be null when the joints acceleration are zero, as states the expression (6).

$$K_x\overline{X} + \dot{\overline{X}} = J^{-1}(\theta)\tau_\theta\ddot{\theta} \tag{6}$$

Therefore, the constant period τ_θ must be as low as possible related to the Cartesian control period T_3.

B. Medium Layer: Passive Wrist Emulator

The scheme which implements the PWE control strategy included in Layer 2 is shown in Fig. 6. This scheme consists on two main blocks shown in the figure as two dotted lines rectangles. The first one represents the abdomen-endoscope interaction, and the second one includes the force control loop for emulating a passive wrist.

The external layer computes the spherical goal coordinate as an arc length L_r and a wrist orientation β_r. The first one is the input of Layer 3 and the second one is used in order to compute the correction γ_r, defined as the absolute reference wrist orientation of the robot.

On the other hand, the force sensor measurements are needed in order to estimate the value of φ_r. It is assumed that the abdomen follows spring behavior [13]-[15]. Thus, a linear relationship exists between F_a and e_a (see Fig. 2 (a)).

In this way, the compensation angle φ_r is obtained using an estimated stiffness λ_e and an estimated *external distance,* ρ_e. Finally, the input F_d is referred to the low limit of acceptable forces measurement, and depends on the noise levels of the sensor itself.

In order to obtain the estimation ρ_e of the real *external distance* ρ, a forces/torques balance has been stated in (7), by using the readings provided by the force sensor, and following the scheme presented in Fig. 2 (a).

$$\begin{cases} \mathbf{R_F} = \mathbf{F} = \mathbf{F_a} + \mathbf{F_r} \\ \mathbf{R_M} = \mathbf{M} = \boldsymbol{\rho_e} \times \mathbf{F} = \boldsymbol{\rho_e} \times \mathbf{F_a} \end{cases} \tag{7}$$

In this balance, the cross product of the external distance $\boldsymbol{\rho_e}$, whose direction matches the endoscope axis, and friction $\mathbf{F_r}$ is null because they are parallel vectors. Applying the norm on torque equation depending on $\mathbf{F}$ (8):

$$M = \rho_e F \sin\psi \rightarrow \left\{ \sin\psi = \frac{F_x}{F} \right\} \rightarrow \rho_e = \frac{M}{F_x} \tag{8}$$

Where the sensor readings $\mathbf{F}=(F_x, F_y, F_z)$, and the angle ψ can be obtained from the cross product between the forces F and F_x. On the other hand, combining the relationship $\mathbf{M} = \boldsymbol{\rho_e} \times \mathbf{F_a}$ from (7) with expression (8), results the following value for F_a (9):

$$M = \rho_e F_a \sin(\frac{\pi}{2} - \beta) \rightarrow F_a = \frac{F_x}{\cos\beta} = \lambda e_a \tag{9}$$

Finally, the conversion of the output force F_x into the compensation angle φ (10) is computed by means of expression (9) and expression (2).

$$F_x = \rho_e \lambda \varphi \tag{10}$$

If the estimation errors of λ_e and ρ_e are closed to zero, then the compensation angle φ_r would assure that the endoscope orientation reaches the initial position of the fulcrum point I_0. However, this is not a real situation, so a PI controller has been added in order to assure no forces are applied to the abdominal wall. The Ackerman's methodology for poles assignment has been used to design the PI control law, according to a dead-beat strategy. In this way, the PI gains can be expressed as follows (11):

$$K_{I2} = \frac{1}{1 - e^{-T_2/\tau}} \quad ; \quad K_{P2} = \frac{\lambda_e(1 + e^{-T_2/\tau})}{(1 - e^{-T_2/\tau})} \tag{11}$$

Where τ is the time constant imposed by the Cartesian controller and T_2 is the control period of this layer.

Finally, the endoscope-abdomen interaction includes the actual abdominal wall spring behavior, as well as the external distance estimator algorithm based on the expression (8). Moreover, this block compensates the endoscope weight in order to simplify the control PI design.

C. External Layer: Spherical Controller

As it has been stated before, the PWE control action changes the endoscope orientation in order to reduce the forced applied to the abdominal wall. In this way, an external spherical control loop is needed in order to recover the desired goal orientation.

Fig. 7 shows this spherical controller (Layer 1) which, using the desired endoscope location β_d, generates a smooth spherical trajectory $\beta_d(kT_1)$, that is used as the PI control law reference. The control loop provides feedback of the real location of the endoscope in order to calculate the required

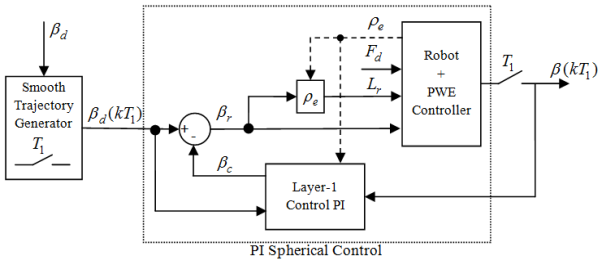

Fig. 7. Spherical controller.

spherical trajectory β_r, eliminating the location error caused by the correction introduced by Layer 2. The Ackerman's methodology for poles assignment has been used to design the PI control law, according to a dead-beat strategy. In this way, the PI gains in Fig. 7 can be expressed as follows (12):

$$K_{I1} = \frac{1}{1-e^{-T_1/\tau}} \quad ; \quad K_{P1} = \frac{1+e^{-T_1/\tau}}{(1-e^{-T_1/\tau})\rho_e} \tag{12}$$

In the previous expression, T_1 is the control period of this layer and τ is the time constant imposed by the Cartesian controller included in Layer 3.

Finally, in order to connect the required spherical trajectory β_r with the inners layers, the arc length L_r has been computed by means of ρ_e.

IV. System Stability

As it has been previously mentioned, the proposed control scheme makes the study of the stability easier, because it is possible to prove the stability on each layer separately.

The Cartesian controller assures the stability on the layer 3, however an study on layers 2 and 3 is needed due to the uncertainties of distance ρ_e and stiffness λ_e.

In this way, the stability of layers 2 and 3 will be focused on their dynamic matrices. For this purpose, it will be considered that those systems are stable when their matrices eigenvalues are below the unit, by means of parameters ρ_e and λ_e. This analysis is easy thanks to the first order dynamic behavior imposed by the Cartesian controller included in the layer 3.

Therefore, dynamic matrices for layers 1 and 2 in closed loop appear in the expression (13).

$$A_1 = \begin{bmatrix} -1 & \rho_e \\ -1/\rho & 1 \end{bmatrix} \quad ; \quad A_2 = \begin{bmatrix} -1 & -1/\lambda_e \\ -\lambda & 1 \end{bmatrix} \tag{13}$$

With the eigenvalues of these matrices, the stability conditions can be expressed as (14).

$$\left| \frac{1}{\rho}\sqrt{\rho(\rho-\rho_e)} \right| < 1 \quad ; \quad \left| \frac{1}{\lambda_e}\sqrt{\lambda_e(\lambda_e-\lambda)} \right| < 1 \tag{14}$$

It can be concluded that the conditions needed for the system to be stable are (15):

$$\rho_e \geq 2\rho \quad ; \quad \lambda_e \geq 0.5\lambda \tag{15}$$

V. Implantation and Experiments

In order to verify the proposed control approach, it has been necessary to carry out some experiments in order to test the appropriate control system operation. A patient simulator has been used for the *in-vitro* procedures, which are required to see how the model responds to artificial, but tangible, tissues. This is the previous step to clinical trials, thus this work does not provides *in-vivo* experimental results. Therefore, the goal of the experiment is testing the proposed control scheme behavior.

The experiment consists of studying the temporal response on an altitude movement that modifies the β angle an interval, for example, from 45 to 30 degrees. The sampling times of each layer are T_1=0.01 seconds for the Cartesian layer, the passive wrist emulation layer is five times slower than the Cartesian, and the same for the Spherical layer. An industrial manipulator (PA-10 by Mitsubishi Heavy Industries, Ltd) with actuated wrist has been used for these tests (see Fig. 8). In order to verify the external distance, a Polaris Optical Tracking System (Northern Digital Inc.) has measured the location of the fulcrum during the experiment. Spherical coordinates α, β and ρ have also been represented to compare the real system with general spherical movement around fulcrum point $\{I_0\}$ in Fig. 1.

A. Navigation with actuated wrist

Fig. 9 (a) and (b) compares the desired orientation α and altitude β with the real values followed by the robot. As it can be noticed, the *real altitude β trajectory* follows the *desired* one in an accurate way. The real trajectory appears to be delayed, but it is an effect of the slow sampling time of the reference.

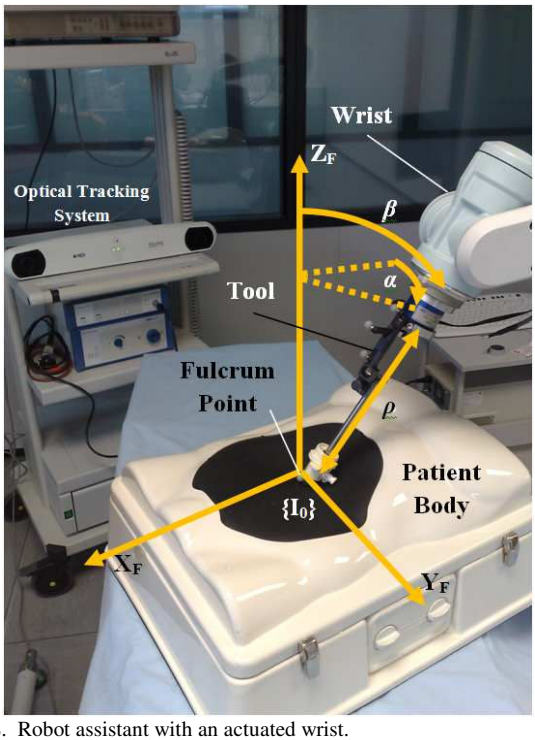

Fig. 8. Robot assistant with an actuated wrist.

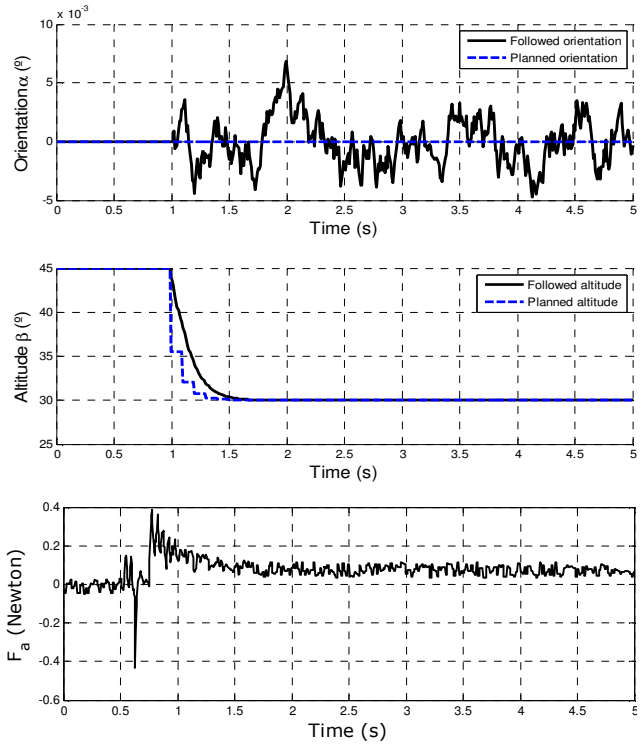

Fig. 9. Orientation α (a), altitude β (b) and abdominal force F_a (c).

B. *Fulcrum point estimation*

Fig. 9 (c) represents the abdominal force when a distance difference exists between the initial fulcrum point I_0 and the actual one. When the endoscope interacts with the abdomen and generates a force and a torque, the control system recalculates the estimated fulcrum point in order to reduce the estimation error. This action reduces the effort applied on the abdomen of the patient. When forces are low, sensor measurements have an intrinsic noise that cannot be avoided. This is the reason why the control scheme must ignore a low-force control.

VI. CONCLUSIONS

This article has described the problem of laparoscopic movement, using a robotic assistant with an actuated wrist. More specifically, the movement on actuated wrists has been developed by emulating the passive mechanism. By studying the results obtained on experiments, it is concluded that behavior of these wrists is very accurate and it produces small errors responses when locating the fulcrum.

Furthermore, actuated wrists could be more attractive for future applications. Since they are capable of applying efforts, with proper modifications on the control scheme, they can be used to other more active tasks. For example: holding an organ, stitch operations and, in general, any action required inside the abdominal cavity.

REFERENCES

[1] P. Berkelman, P. Cinquin, J. Troccaz, et al. "State-of-the-Art in Force and Tactile Sensing for Minimally Invasive Surgery". IEEE Sensors Journal (April 2008), Vol. 8, No.4, pp. 371-381.

[2] R. Hurteau R., S. DeSantis, E. Begin, M. Gagner, "Laparoscopic Surgery Assisted by a Robotic Cameraman: Concept and Experimental Results". Proc. of 1994 IEEE International Conference on Robotic & Automation. San Diego, California, USA (1994), pp. 2286-2289.

[3] B. Pan, Y. Fu and S. Wang. "Position Planning for Laparoscopic Robot in Minimally Invasive Surgery". Proc. of 2007 IEEE International Conference Mechatronics and Automation. Harbin, China (August 2007), pp. 1056-1061.

[4] N. Zemiti, T. Ortmaier, G. Morel. "A New Robot for Force Control in Minimally Invasive Surgery," Proc. of 2004 IEEE International Conference on Intelligent Robots and Systems. Sendai, Japan (2004).

[5] N. Zemiti, G. Morel, T. Ortmaier, and N. Bonnet. "Mechatronic Design of a New Robot for Force Control in Minimally Invasive Surgery". IEEE Transactions on Mechatronics. Vol. 12, No. 2, (April 2007), pp. 143-153.

[6] V.F. Muñoz, I. García-Morales, et al. "Control movement scheme based on manipulability concept for a surgical robot assistant". Proc. of 2006 IEEE International Conference on Robotic & Automation. Orlando, FL (2006), pp. 245-250.

[7] G. Niemeyer, N. Swarup, et al. "Camera referenced control in a minimally invasive surgical apparatus". World patent WO0060521 (2000).

[8] Y. Wang, K. Laby. "Automated endoscope system for optimal positioning". USA patent US5815640 (1998).

[9] P. Berkelman, P. Cinquin, J. Troccaz, et al. "A Compact, Compliant Laparoscopic Endoscope Manipulator". Proc. of 2002 IEEE International Conference on Robotic & Automation. Washington, DC (2002), pp. 1870-1875.

[10] E.G. Christoforou, N.V. Tsekos. "Robotic manipulators with remotely-actuaded joints: Implementation using drive-shafts and u-joints". Proc. of 2006 IEEE International Conference on Robotic & Automation. Orlando, FL (2006), pp. 2866-2871.

[11] M.J.H. Lum, J. Rosen, et al. "Optimization of a Spherical Mechanism for a Minimally Invasive Surgical Robot: Theoretical and Experimental". IEEE Transactions on Biomedical Engineering, Vol. 53, No. 7, (July 2006), pp. 1440-1445.

[12] T. Suzuki, Y. Katayama et al. "Compact Forceps Manipulator for Laparoscopic Surgery". IEEE Conference on Intelligent Robots and Systems, 2005, pp. 3678-3683.

[13] P. Huang, L. Gu, J. Zhang, X. Yu, et al. "Virtual Surgery Deformable Modelling Employing GPU Based Computation". 17th International Conference on Artificial Reality and Telexistence. Aalborg University Esbjerg, Denmark (2007), pp. 221-227.

[14] A. Rahman, U. H. Khan. "Effect of Force on Finite Element in Vivo Skin Model". Second IEEE International Conference on Emerging Technologies (ICET 2006). Peshawar, N-W.F.P, Pakistan (2006), pp. 727-734.

[15] N. Nakamura, M. Yanagihara et al. "Muscle Model for Minimally Invasive Surgery". IEEE International Conference on Robotics and Biomimetics, 2006, pp. 1438-1443.